Published in final edited form as:
Neuron. 2009 August 27; 63(4): 508–522. doi:10.1016/j.neuron.2009.07.016.

Direct activation of sparse, distributed populations of cortical neurons by electrical microstimulation

Mark H. Histed[*], **Vincent Bonin**, and **R. Clay Reid**[*]
Department of Neurobiology Harvard Medical School 220 Longwood Ave. Boston, MA 02115

Summary

For over a century, electrical microstimulation has been the most direct method for causally linking brain function with behavior. Despite this long history, it is still unclear how the activity of neural populations is affected by stimulation. For example, there is still no consensus on where activated cells lie, or on the extent to which neural processes such as passing axons near the electrode are also activated. Past studies of this question have proven difficult because microstimulation interferes with electrophysiological recordings, which in any case provide only coarse information about the location of activated cells. We used two-photon calcium imaging, an optical method, to circumvent these hurdles. We found that microstimulation sparsely activates neurons around the electrode, sometimes as far as millimeters away, even at low currents. The pattern of activated neurons likely arises from the direct activation of axons in a volume with a diameter of tens of microns.

Introduction

The ability to change the activity of neurons and measure the consequent effects is critical to a full understanding of the brain. Electrical stimulation affects neural activity by affecting the voltage gradient that neurons maintain across their membranes; a current passed outside of cells can change this voltage and trigger neuronal responses. This technique was first used in the 19th century by Fritsch and Hitzig (1870), who stimulated the brains of dogs and identified the motor cortex, from which movements could be elicited, thus showing that the brain was divided into different functional areas. Subsequent stimulation experiments in motor cortex of humans (Penfield, 1947) and monkeys (Asanuma et al., 1968) identified a motor homunculus: an orderly mapping of the muscles of the body onto the cortical surface. Stimulation has also been long used to map neural connections between brain regions (Bishop et al., 1962; Bizzi, 1967; Movshon and Newsome, 1996; Sommer and Wurtz, 2002).

The ability of stimulation to change neural activity allowed Newsome and colleagues (Salzman et al., 1992) to link neural firing in cortical area MT with visual motion perception. Similarly, electrical stimulation has been used to modulate attention (Moore and Fallah, 2001), to increase the speed of learning (Williams and Eskandar, 2006), to identify neural subtypes (Sommer and Wurtz, 2002), to reorder movement sequences (Histed and Miller, 2006), to study

[*]To whom correspondence should be addressed. Department of Neurobiology Harvard Medical School 220 Longwood Ave. Boston, MA 02115 mark_histed@hms.harvard.edu Phone: +1 (617) 432-3621. [*]Department of Neurobiology Harvard Medical School 220 Longwood Ave. Boston, MA 02115 clay_reid@hms.harvard.edu Phone: +1 (617) 432-3621.
vincent_bonin@hms.harvard.edu

somatosensory perception (Romo et al., 1998), and, combined with fMRI, to map connections (Tolias et al., 2005; Ekstrom et al., 2008; Moeller et al., 2008). Finally, recent steps toward brain-machine interfaces propose the use of electrical stimulation to introduce signals directly into the brain (Schmidt et al., 1996; Chapin, 2000; Lebedev and Nicolelis, 2006; Tehovnik and Slocum, 2007; Pezaris and Reid, 2007; Fitzsimmons et al., 2007; Schiller and Tehovnik, 2008).

However, all of this work is limited by the fact that the identity of neurons affected by stimulation remains unknown. As an example, the motor homunculus' relation to motor cortex function is still debated. Some studies have suggested that the homunculus is an artifact of stimulation on the basis of the substantial differences between recorded neural responses and the muscles activated by stimulation at the same site (for discussion, see: Graziano et al., 2002a; Strick, 2002; Graziano et al., 2002b; Rathelot and Strick, 2006).

The predominant idea in the field is that stimulation leads to a sphere of activated neurons around the electrode tip that increases in size with increasing current (Stoney et al., 1968; Robinson and Fuchs, 1969; Ranck, 1975; Tehovnik, 1996; Murasugi et al., 1993; Tolias et al., 2005). This hypothesis is based on the data of Asanuma and colleagues (Stoney et al., 1968), who estimated that 10 μA and 100 μA currents activated cells in a radius of 100 μm and 450 μm around the electrode (cited by e.g. Bruce et al., 1985; Salzman et al., 1992; Murasugi et al., 1993; Tehovnik, 1996; Moore and Fallah, 2004; Tolias et al., 2005).

However, this idea — that larger currents activate neurons at a larger distance from the electrode — is based on few studies, because of two central difficulties. First, it is impossible to record and stimulate electrically nearby at the same time, due to artifacts from the high voltages used in stimulation. This led Stoney et al. (1968), for example, to use an indirect measure of neural activation based on the interference between action potentials evoked by stimulating the cortex locally and stimulating distant cortical axons. The difficulty of this approach has largely prevented follow-up work. Second, because each recording electrode can only sample a small number of neurons, there is a needle-in-a-haystack problem of finding the neurons activated by stimulation. For example, while chronaxie measurements suggest that axons have the lowest threshold (Ranck, 1975; Nowak and Bullier, 1998a; Tehovnik et al., 2006), it is not clear whether initial segments have lower thresholds (especially for cortico-cortical axons which are often unmyelinated, e.g. Tehovnik et al., 2006; Nowak and Bullier, 1998b), which would cause preferential activation of cells near the electrode tip.

The optical technique of two-photon calcium imaging of networks of neurons (Stosiek et al., 2003; Ohki et al., 2005; Kerr et al., 2005; Kerr and Denk, 2008) solves both these problems. Optical measurements of neural activity are independent of electrical stimulation, and allow for imaging of hundreds of neurons in a single plane around the electrode tip.

Using this technique, we found that microstimulation directly activates a sparse, distributed population of neurons. Stimulation activated cells hundreds of microns from the tip, even near threshold (4–9 μA), without a strong bias for neurons near the tip. The pattern of activated cells was sparse; instead of activating cells at greater distance, we found that increasing current fills in a large sphere of activated cells. The mechanism of activation was local and direct; moving the electrode by 30 microns completely changed the patterns of activated cells and blocking excitatory transmission had little effect on the patterns of activation.

These data thus suggest an alternative model for how neurons are activated by electrical stimulation. Instead of activating a group of cell bodies that increases in size as current is increased, we propose that stimulation activates a much smaller volume of neural processes around the electrode tip. The result is a sparse and widely distributed set of activated cell bodies whose pattern is highly sensitive to the exact location of the electrode in the neuropil.

One immediate implication is that it is impossible to activate a set of cells restricted to a small spatial volume, which may explain why stimulation has principally been successful in areas like macaque visual area MT (Murasugi et al., 1993) where neurons of similar function lie near one another. These results promise to recast the interpretation of past studies that have used microstimulation to affect brain and behavior, and outline ways in which microstimulation might be used in new experiments to study neural circuits.

Results

We used two-photon calcium imaging to determine the locations of the neurons activated by cortical microstimulation. We imaged layer 2/3 of visual cortex in the rodent (rat and mouse, area 17) and cat (area 18) while stimulating in the same area (Fig. 1A,B). We labeled neurons and astrocytes with the calcium indicator Oregon Green BAPTA-1 AM (OGB-1) in a region of 100–600 μm in diameter using the method of Stosiek et al. (2003; Ohki et al. 2005, 2006), and co-labeled astrocytes with a red dye, sulforhodamine 101 (SR-101, Nimmerjahn et al., 2004; Schummers et al., 2008). A single imaged plane from cat visual cortex (Fig. 1B) illustrates neurons (green), astrocytes (yellow or red), and blood vessels of various sizes (black). Between these features are areas of labeled neuropil (dim green).

From past studies (Smetters et al., 1999; Kerr et al., 2005; Sato et al., 2007; Greenberg et al., 2008), we know that somatic calcium in cortical neurons largely reflects action potential firing, rather than subthreshold events. To a first approximation, the time course of somatic calcium concentration is the linear convolution of the spike train with the single-spike calcium response, which has a rapid rise and a slower exponential decay (Fig. 1C, Helmchen et al., 1996; Yaksi and Friedrich, 2006; Greenberg et al., 2008). For high spike rates, fluorescence responses can saturate, depending on the concentration and affinity of the indicator loaded into the cells (Helmchen et al., 1996). We therefore limit our analysis to the detection, rather than quantification, of the large changes in fluorescence evoked by trains of electrical pulses.

We typically positioned the electrode within the imaged region at the same depth as the imaging plane (Fig. 1B). In some experiments, we also looked for long-range effects by placing the electrode some distance away (1–4 mm). We stimulated with both metal electrodes made of tungsten and Pt-Ir, and glass pipettes, which are thinner and thus deform and damage the tissue less than metal electrodes.

Our stimulation protocols matched protocols used in previous studies of the influence of cortical circuits on behavior. We used constant-current biphasic square pulses, each phase lasting 200 μs, with the negative pulse first (reviewed in Ranck, 1975; Tehovnik 1996) at 250 Hz in trains of 100 to 815 ms. We concentrated on low currents (10 μA or lower), which have been used in perceptual studies in visual cortical areas (Salzman et al., 1990; Murphey and Maunsell, 2007; Bak et al., 1990; Tehovnik and Slocum, 2007), rather than on the higher currents (~10–50 μA) that have typically been used to evoke motor outputs (i.e. Bruce et al., 1985; Graziano et al., 2002a). By directly activating fewer cells, we hoped to minimize the effect of synaptic activation on our measurements. We also used near-threshold currents to minimize inhibitory recruitment (Creutzfeldt et al., 1966; Berman et al., 1991; Chung and Ferster, 1998; Kara et al., 2002), and avoid axonal block effects (Durand, 2000). Thus, this work preferentially examines the direct mechanisms of neuronal activation by stimulation.

Activation is sparse and distributed

In response to stimulation near threshold, we observed that some cells were strongly activated while other nearby cells did not respond (Fig. 2B,E). Astrocytes typically showed no fluorescence changes, perhaps because they respond only following large firing events in many nearby neurons (Schummers et al., 2008). When we collected data at high frame rates (31 Hz),

we were able to resolve the rising phase of the response to a 100 ms train (Fig. 2F). In the best experiments, we could even resolve responses in individual trials (Fig. 2C,G).

By imaging all the neurons in a single plane around the electrode tip, we found that stimulation at threshold reliably activated a sparse, distributed set of neurons (Fig. 3). Some of these activated neurons were located hundreds of microns away from the tip, yet only a small fraction of all neurons were activated. Results obtained for metal electrodes (Fig. 3A) and glass pipettes (Fig. 3C) were qualitatively similar. Based on the fact that activated cells produced large responses of 20–30% (change in fluorescence relative to baseline fluorescence, $\Delta F/F_0$, see Methods; Supp. Figs 2,5), we identified cells showing greater than 20% response over a 0.75 to 1-second period after stimulus train onset as showing significant responses to stimulation (Fig. 3B). We used a constant $\Delta F/F_0$ threshold so that we could compare experiments with different optical properties and thus different signal-to-noise ratios. In all experiments, this threshold was well above the empirical noise floor such that the responses to stimulation were reliably detected (Fig. 2, Supp. Figs. 2,5).

Activation thresholds were generally low (Fig. 3D), and in the range previously used to elicit behavioral responses. In a set of experiments (N=8) from each species we estimated the number of activated cells with increasing current. The current needed to activate at least one cell was 10 μA or less. By comparison, currents required to evoke saccades from frontal lobe areas and the superior colliculus are typically between 12 and 50μA (Bruce et al., 1985;Schlag and Schlag-Rey, 1987;Stanford et al., 1996). Some work in motor cortex has used currents in that range (Graziano et al., 2002a), and other experiments have seen muscle twitches at currents at 5–10 μA (reviewed in Taylor and Gross, 2003). In MT, the Newsome group showed that 10 μA in one-second trains could produce biases in direction discrimination without evoking overt movements (Salzman et al., 1990;Salzman et al., 1992). Finally, in cases where animals are asked to detect the presence of stimulation, thresholds are often below 10 μA (Doty, 1969;Murphey and Maunsell, 2007).

In the cat but not in the rodent, lateral axons are known to extend over several millimeters within layer 2/3 of visual cortex (Gilbert and Wiesel, 1979; Rockland and Lund, 1982; Martin and Whitteridge, 1984; Gilbert and Wiesel, 1989; Gilbert, 1992). In two experiments in the cat, we found that neurons up to 4 mm away from the stimulation site could be activated with currents as low as 10 μA (Fig. 3E). In all three species, we observed similar sparse patterns of activation and similar thresholds (Fig. 3C). We proceeded to investigate the mechanism by which these sparse patterns arose by doing further experiments in mouse cortex.

Stimulation activates neural elements in a small volume around the tip

We considered two possibilities to explain the sparse activation near threshold. First, sparse activation could arise from cell bodies having different thresholds. The activated neurons might be those with the lowest thresholds to stimulation such that, as we increased current, neurons with successively higher thresholds would be recruited. Alternatively, cell processes could be activated very locally. The activated neurons might simply be those whose axons or dendrites pass through a small volume near the tip.

We can distinguish between these hypotheses by moving the electrode tip by small amounts and looking at the resulting patterns of activation. If cell bodies far away from the electrode are activated directly, then moving the electrode a short distance should barely change the applied voltage at distant cells and a similar pattern of activation should be observed. On the other hand, if stimulation has primarily local effects on cell processes, then the patterns of activated cells should depend strongly on electrode position.

We found support for the latter hypothesis: stimulation had a very local effect near the tip, even though the activated cells were widely distributed (Fig. 4). We measured the patterns of activation near threshold before and after moving the tip 15 μm and observed that distinct population of cells were activated (Fig 4B–C), with only a few activated cells common to both stimulation sites. Stimulation with higher current activated more cells (Fig. 4D), with more cells common to both sites, suggesting the activation of a larger volume of processes around the tip. To confirm that tip position is the key determinant of which cells are activated, we moved the electrode and then repositioned it to its original location (Fig. 4E). In this experiment, we found that some neurons are activated at the first position both before and after the movement, but not in the second, deeper, position.

Finally, to quantify the size of the activated volume, we moved the electrode tip incrementally and measured overlap with the cells activated at the initial position. We found that, at low currents, moving the electrode tip 30 μm almost completely eliminated overlap of activated neurons (Fig. 4F), indicating that stimulation excited neural processes within a radius of 15 μm (Fig 4F).

Direct versus synaptic activation

We next wished to determine whether our stimulation trains were directly activating cells (i.e. through passive current spread: Stoney et al., 1968; Bruce et al., 1985; Moore and Fallah, 2004), or whether many of the responses were due to postsynaptic effects, in which directly activated cells were driving other cells to spike. Most connections between two cells in the cortex are relatively weak (Galarreta and Hestrin, 1998; but see Silver et al., 2003) and so a pre-synaptic neuron's spike produces a spike in its postsynaptic partners only rarely (Ts'o et al., 1986). Although we stimulated only a small proportion of cells near threshold, we nonetheless wished to rule out the possibility that the responses were dominated by synaptic connections.

In order to distinguish between these two possibilities, we used pharmacological agents (CNQX and APV) to block excitatory glutamatergic transmission and measured the effects of stimulation before and after (Fig. 5). As a positive control for the blockade, we interleaved visual stimuli with electrical stimuli while applying the drug and then washing it out.

We found the sparse patterns of activation observed at threshold to be largely independent of synaptic transmission (Fig. 5). Responses to electrical stimulation were generally unaffected by application of CNQX and APV (Fig. 5A–C). In contrast, visual responses were almost totally eliminated, suggesting complete blockade of synaptic transmission. These results hold both for somatic calcium signals (Fig. 5A–B, E), and for the average of cell bodies and surrounding neuropil (Fig. 5C–D). Because wash-in and wash-out could take as long as 90 min, and any small shift of the brain during that time would cause small tip movement and change the activated population (see above), we could not ensure that the exact same set of cells were excited throughout. However, in one experiment we were able to make this comparison for a small number of neurons (Fig. 5E).

These results show that even under blockade of excitatory synaptic transmission, many cells are strongly activated by electrical microstimulation. These cells are thus activated via direct depolarization. While we cannot completely rule out some degree of synaptic activation under control conditions, the proportion of activated cells is similar under control conditions and synaptic blockade.

Cellular versus neuropil responses

While the cell bodies of neurons are identifiable in the images resulting from two-photon bulk-loaded calcium imaging, the regions between the neurons are also loaded with calcium indicator. This neuropil region contains many neural processes --- axons and dendrites --- that are below the resolution limit of optical microscopes. We have observed cells that show large responses and also cells that show little or no response to stimulation. Since the neuropil is composed of the processes of the surrounding cells, we might expect it to respond like a spatially-averaged version of the cells. That is what we observed (Fig. 6A). Activated and non-activated cells are embedded in a surrounding region of weakly activated neuropil, but by selecting the cells by their shape, one can largely isolate neuropil and cell responses (Fig. 6B–D).

Since activated cells are widely dispersed, we expected the neuropil signal to be non-zero even at large distances, and that was the case (Fig. 7). Here, in an experiment where the electrode was positioned at the edge of the field of view, we stimulated with two different currents, 10 μA, near threshold, and 25 μA, well above threshold. The neuropil response is very strong in a small region around the electrode tip, but falls off slowly at greater distances, without approaching zero within the imaging field of view (Fig. 7B).

Discussion

We found that stimulation near threshold produces a sparse and distributed set of activated cells around the electrode. The effects of stimulation are very local, so that moving the tip by as little as tens of microns changes the cells that are activated, implying that we are activating neural processes that run near the tip (Fig 8A). This leads to a large and sparse region of activated cell bodies, even at low current (Fig. 8B).

This model provides a clearer understanding of how stimulation actually recruits neurons. Previous work relied on the idea that increasing current activates neurons whose cell bodies are located at an increasing distance from the tip (e.g. Stoney, 1968; also see *Introduction*). While that may be a weak effect, our data shows that by far the most prominent effect is that increasing current instead fills in a large region of activated neurons. The pattern of activated cells, moreover, is likely to reflect the pattern in which axons project through the cortex.

Below, we discuss how cells may be activated through their processes, and explain why little postsynaptic activation is seen in the near-threshold regime we explored. We discuss some details of methodology related to stimulation and to imaging, specifically with respect to distinguishing signals from cell somata and the surrounding neuropil. We consider the various types of electrical stimulation used in the brain *in vivo* and outline how these relate to our work. Lastly, we discuss how the wide spatial distribution of activated neurons might bears on future basic and clinical studies.

Types of neural elements activated

An open question is what types of neural elements mediate this very local activation (Fig. 8C). We think that near threshold activation is mediated primarily by axons (as opposed to dendrites), for three reasons. First, dendrites do not extend far enough laterally to explain the activation of many cells hundreds of microns or more from the tip. The maximal radius of basal dendrites is typically 100 μm, while axons can extend 500 μm or more (Braitenberg and Schüz, 2001). Distant cells responded similarly to those located 100 microns or less from the tip; they had similar threshold, fluorescence change, and response reliability. Second, axons have lower thresholds than cell bodies or dendrites (Stuart et al., 1997;Ranck, 1975;Tehovnik, 1996) in response to the effective current injection produced by extracellular stimulation (Durand,

2000;Rattay, 1999;Merrill et al., 2005). Third, axons conduct action potentials without loss even if that action potential is induced externally, whereas dendrites are not always perfectly regenerative conductors (Stuart et al., 2000). Thus, while some cells might be activated through their dendrites at higher currents, axons are likely to be recruited first. Data on chronaxies (asymptotes of the strength-duration curve) support the idea that axons are the main neural elements activated by stimulation (Nowak and Bullier, 1998a;Tehovnik et al., 2006).

External stimulation of an axon produces two effects. The induced action potential travels both backward to the cell body and forward to the synaptic terminals (Bishop et al., 1962; Lemon, 1984). At the soma, this causes calcium influxes that we measure. At the presynaptic boutons, it can cause synaptic release.

Stimulation drives a small number of cells strongly

We typically observed several neurons, even at low, near-threshold currents, that showed a very large fluorescence change. The cells that show large fluorescence changes, even at low stimulation currents, are likely to be driven directly to spike many times by microstimulation trains, as discussed further below (*Calcium imaging*). However, while we did analyze these in detail in this report, some cells respond with lower fluorescence changes (e.g. Fig. 6D), which may correspond to fewer induced spikes. These cells may be driven postsynaptically by the strongly driven cells, they may be sectioned incompletely by the imaging plane, or they may be driven weakly by direct depolarization from the stimulation. If driven directly, their processes may lie farther from the tip than the strongly-driven cells, or they may be driven through their dendrites. Also, while Fig. 4 and Supp. Fig. 8 show that different processes and thus neurons are activated by moving the tip, we cannot completely rule out variations in current threshold across neurons and axons. Indeed, it is known that smaller diameter axons have higher thresholds than large axons (Ranck, 1975). However since many cells appear to be driven very strongly (i.e. show large reliable $\Delta F/F_0$ changes; Figs. 2,6;Supp Figs 2, 6, 10), it is possible that the slope of the current-activation curve is very steep, yielding an essentially all-or-nothing response (cf. Huber et al., 2008).

Effects on synapses: implications for driving postsynaptic responses

To understand how microstimulation affects the cortex, we studied how cells are directly affected by the applied current. Our goal was to understand the mechanism by which spikes are induced in the cortex by stimulation. However, this directly-activated set of neurons has effects on other neurons via synaptic connections. Indeed, previous work has shown that cortical stimulation can produce postsynaptic spiking (Stoney et al., 1968; Butovas, 2003).

In our experiments, postsynaptic effects were far weaker than direct effects. There are several possible explanations for this. First, we used low currents. Larger currents recruit more neurons, producing more opportunity for postsynaptic summation to result in spikes. Also, it is known that larger currents can recruit inhibitory neurons (Creutzfeldt et al., 1966; Chung and Ferster, 1998; Kara et al., 2002). Second, synapses in the cortex are typically weak, and many pre-synaptic inputs are required to produce a spike in a postsynaptic cell (Häusser et al., 2001; Galarreta and Hestrin, 1998). Finally, synaptic depression is often seen in the cortex (Varela et al., 1997; Deisz and Prince, 1989; Stratford et al., 1996; Thomson and Deuchars, 1994), and while single stimulation pulses might thus cause the largest postsynaptic effects, we used typical high-frequency microstimulation trains that would be likely to induce depression and decrease postsynaptic spiking.

Future cortical microstimulation studies should consider three potential effects on synapses. First, the early pulses in a train are likely to have the biggest effect. This is consistent with a study that found that spacing early pulses as widely as possible had a stronger effect on eye

movements (Kimmel and Moore, 2007), presumably by reducing synaptic depression at the start of the train. Second, synaptic effects will be stronger at facilitating synapses than at depressing synapses. It may be that, for example, subcortical projections out of an area facilitate more than cortico-cortical projections. Third, synaptic recovery should be considered. The end of a stimulation train may leave synapses of stimulated cells in a very depressed state, causing them to have a weaker effect on the circuit right after stimulation than before the stimulation train.

Electrical stimulation and *in vivo* calcium imaging

Because one has tight control over the neural elements being activated, electrical stimulation can be a simple method for understanding and calibrating *in vivo* two-photon calcium imaging. Microstimulation combined with imaging can provide an empirical measure of the degree to which neuropil responses may mix with and contaminate somatic signals (Fig. 6). Future work may exploit the relative homogeneity of neuropil response that we observed (Fig. 7) to measure contamination under imaging conditions specific to a particular preparation or microscope. Thus, while we have used imaging to calibrate responses to stimulation, these data can in part be useful to calibrate imaging.

Cells that are almost completely above or below the imaging plane will contain components of the neuropil signal below or above them, because the two-photon imaging plane is not infinitely thin. This would not affect our results, as we mainly study cells which show 20% or greater changes in fluorescence. Since the neuropil is relatively homogenous and shows less than a 10% change through most of the field of view (Figs. 6 and 7), any neuropil contribution would only dilute stimulation-induced somatic fluorescence changes.

The relationship between neuronal spiking and the fluorescence signal we measured could be complicated by possible saturation of the calcium indicator's response. In an indicator's linear range — which depends on the baseline cellular calcium concentration, endogenous buffering, and indicator affinity — fluorescence responses from several spikes will combine additively to produce a large change with the same decay constant (Helmchen et al., 1996; Yaksi and Friedrich, 2006). Saturation of the indicator would cause reponses to sum sub-linearly. This does not materially affect our results because it would only cause responses to be smaller than expected for a given number of spikes, not larger.

We frequently observed changes in fluorescence of 20–30% or more as a result of stimulation. Several other laboratories have seen 3–8% changes in fluorescence per spike with OGB-1 AM (Kerr et al., 2005; Greenberg et al., 2008; Sato et al., 2007), and while some variation arises from differences in intracellular dye concentration and background fluorescence, we have observed 4–6% changes in response to single pulses (Supp. Fig. 1). Our large observed fluorescence changes thus are a result of at least several somatic spikes, and probably more, because indicator saturation will tend to cause spike numbers to be underestimated. Stimulation responses are also large compared to visual responses (e.g. Fig. 5, see also Ohki et al., 2005).

Regimes of electrical stimulation in cortex

Past work has used stimulation at a variety of currents. Some are low, similar to our near-threshold levels (as low as 10 μA), used primarily to modulate perception (Salzman et al., 1992; Moore and Fallah, 2004; Glimcher and Sparks, 1993) or when animals were trained to detect minimal current (Doty, 1969; Murphey and Maunsell, 2007). Other past studies have used higher currents (up to 50 μA), often to evoke immediate motor behavior (Bruce et al., 1985; Graziano et al., 2002a). Our results may provide insight into both regimes.

At low currents, we found that neurons are primarily driven directly, rather than synaptically. To produce any behavioral effects, however, some synaptic responses must result from stimulation. But these postsynaptic responses are likely weak relative to direct drive, and since only a small number of spikes are required to produce a behavioral effect (Houweling and Brecht, 2008), even weak postsynaptic effects could change behavior. Thus, our data suggest that low currents (as used e.g. by the Newsome lab in cortical area MT) result in activation of a set directly driven neurons which induce only a small number of spikes in their connected partners.

At higher currents, we found that larger populations of neurons are driven directly (Fig. 5; Supp. Fig. 4). Other neurons may be activated because of summation of many inputs from the direct population. Thus, postsynaptic effects may play a relatively more important role than in the near-threshold regime discussed above. In areas such as the frontal eye fields, the threshold to evoke a movement can be as low as 10 μA but is sometimes as high as 50 μA (Bruce et al., 1985). It is possible that these higher behavioral thresholds reflect the point where enough postsynaptic effects occur to trigger a coordinated network event resulting in a motor output. It may also be the case that the postsynaptic summation actually occurs in sub-cortical areas to which stimulated axons project. Further work is needed to resolve this issue, and as connection patterns specific to an area are likely to be important, future studies should be targeted to specific cortical areas.

We note that microstimulation is very different from deep brain stimulation (DBS), which is widely used in treatment of Parkinson's disease and other disorders. DBS electrodes have a much greater surface area than microstimulation electrodes and thus produce a very low current density at their electrode surfaces (Johnson et al., 2008; Vitek, 2002), Another clinical stimulation technique is bipolar cortical surface stimulation (Desmurget et al., 2009), which our data suggest may induce spikes in axons of the tissue nearest the electrode, cortical layer I. It would be of considerable interest to extend the techniques used here to study these therapeutic stimulation techniques.

Microstimulation affects groups of cells spread over the cortex: implications for future studies

This work raises several issues to consider for the design and interpretation of microstimulation studies as well as for future clinical applications.

First, our results indicate that it is nearly impossible to stimulate single cells using microstimulation. We found that a change in current of 1–2 μA often changed the number of visible cells activated from zero to five or more. Moreover, we have imaged only a single plane – a single slice through a sphere of several hundred microns in diameter around the tip – and it is likely that many cells at different depths were also activated by stimulation (cf. Göbel et al., 2007). This implies that extracellular microstimulation is highly unlikely to ever activate a single cell, although this can be done with juxtacellular (or cell-attached) stimulation (Houweling and Brecht, 2008), where the pipette tip is specifically pressed against the cell's membrane. Also, iontophoretic application of glutamate can activate a small number of cells near the pipette tip (Garaschuk et al., 2006), though both this and juxtacellular stimulation are more technically difficult than microstimulation *in vivo*.

Second, we found that microstimulation is extremely sensitive to small motions of the tip. The small region of activated processes means that any motion can dramatically change the set of stimulated cells. Experiments which require very consistent effects on the same cells therefore will require exceptional electrode stability (e.g. Ekstrom et al., 2008), which may be difficult or impossible to achieve in practice.

Third, the pattern in which cells are activated will depend on projection patterns in the cortex. Different cortical areas with different axonal anatomy and projection patterns may thus respond differently to stimulation. For example, in the visual cortex of cats where columns of the same orientation preference are preferentially connected (Gilbert and Wiesel, 1989), or potentially in the direction columns of MT (Albright et al., 1984), high-current stimulation may activate a set of connected columns. Most behavioral effects of microstimulation have been in areas with known columnar architecture, possibly because cells of similar functional properties lie near one another and are therefore activated together.

Fourth, the cells whose responses are recorded on an extracellular electrode are likely to be different than the cells activated when stimulating through that electrode. Extracellular recording mainly reveals large current flows (Johnston and Wu, 1994; Henze et al., 2000) coming from the somata of neurons near the electrode. However, we found that stimulation through that electrode drives distant cells. Again, experiments exploiting microstimulation may require brain regions where cells of similar function are grouped together.

Finally, our data has important implications for brain-machine interfaces and cortical prosthetics. For example, visual prosthetics may someday restore sight to those with damaged retinas by using a camera to record the visual world and stimulating the visual cortex or visual thalamus (Schmidt et al., 1996; Pezaris and Reid, 2007; Schiller and Tehovnik, 2008). Because stimulation of a single site in the cortex activates neurons that are spread widely from that site, achieving high-resolution rasterized visual percepts by electrical stimulation through high-density electrode arrays may not be possible, unless the brain can learn to interpret these distributed patterns (e.g. Jackson et al., 2006; Murphey and Maunsell, 2007; Murphey and Maunsell, 2008).

Conclusion

Over its long history, electrical microstimulation has given us great insight into brain function. Its applicability has nonetheless been limited by a lack of understanding of its effects on individual neurons, and the optical technique we have used has yielded a new understanding of these effects. But this work could not be, and is not, a complete study of the many uses of stimulation across different organisms, brain regions, and behavioral contexts. Our principal result is that microstimulation creates a sparse and distributed pattern of activated neurons through axonal activation. Because cortical anatomy shares common features across brain regions and species (Douglas and Martin, 1998), this result is likely to generally apply across different types of cortex in different species. Specifically, in humans, the application of these techniques to clinical stimulation procedures also promises improvements in the therapeutic use of electrical stimulation.

Experimental Procedures

Animal preparation and surgery

All procedures were conducted in accordance with the ethical guidelines of the National Institutes of Health and were approved by the IACUC at Harvard Medical School. Experiments were performed in mice (C57/Bl6; N=12), rats (Long-Evans; N=3), and cats (N=8). We imaged cat visual cortex to examine effects of known long-range axonal projections. Animals ranged in age from P30 to P150. Anesthesia in cats was induced with ketamine and acepromazine and animals were maintained on isoflurane (1.0–1.5%), without paralysis. Rodents were anesthetized with a combination of fentanyl, medetomidine and midazolam (Mrsic-Flogel et al., 2007). Animals' vital signs were monitored and temperature was maintained within a physiological range. Depth of anesthesia was monitored by EEG and/or by assessing the response to a toe pinch. A craniotomy was made (2–4 mm in diameter), in some cases the dura

was removed to improve optical properties, and agarose (1.5–3%; type III-A, Sigma-Aldrich) was placed on top of the brain to suppress physiological motion. In some cases a cover glass (World Precision Instruments) was used above the agarose to further reduce motion.

We injected dye solution containing Oregon Green BAPTA-1 AM (Invitrogen) with 10% DMSO and Pluronic F-127 in ACSF (Stosiek et al., 2003) approximately 200 μm below the surface, using either a 2 min pulse or 40–80 short pulses. The injection solution also contained 50–100 μM sulforhodamine-101 (Nimmerjahn et al., 2004) to label glial cells. Both neurons and glia were labeled with OGB-1, likely because we injected large volumes of dye in an effort to label as large a region as possible. Data collection began 30–60 min after injection.

CNQX (500 μM; Invitrogen) and d-APV (1.5 mM; Sigma-Aldrich) in ACSF (pH 7.4, 320 mOsm) were applied either in the objective immersion fluid bath above the agarose covering the brain and dura, or by injecting near the imaging site through a pipette (1–4 psi). We began the washout by rinsing several times and then replacing the immersion fluid with ACSF.

Stimulation

We stimulated with electrodes made of tungsten (A-M Systems) or platinum-iridium (Nanobioprobes, Israel; FHC, Bowdoinham, ME), or used a glass pipette with a broken tip of outer diameter 3–5 μm filled with ACSF with or without dye. Glass pipettes were used particularly for experiments in which the tip was moved because they deform the tissue less than metal electrodes; they also appeared to produce less tissue damage. Once sited in the tissue, pipette solution was stably retained in the tip, and was not expelled by stimulation with our charge-balanced pulses (but could be expelled iontophoretically by steady current injection). After stimulation, metal electrode tip impedances were 100–500 kOhm, and tip sizes were between 10 μm–50 μm. Pipette impedances were between 5 and 15 MOhm. We used trains of 100 ms or 815 ms length composed of short pulses at 250 Hz, beginning 100 ms before the frame on which stimulated responses were computed. Constant-current pulses were provided by a stimulus isolator (A-M Systems; Bak Instruments), and pulses were charge balanced. Total loop capacitance was less than 30 pF. Stimulation was monopolar and the return was a low-impedance metal connection to the skull. Electrodes were positioned with a micromanipulator (Sutter Instruments MP-285). In several cases, we pseudo-randomly intermixed the order of trains of different current and saw no effect on the responses (data not shown), which indicates that there were no long-term interactions from one train to the next. In Fig. 3, train length was 815 ms in the three metal electrode experiments (all of which had thresholds of 7.5 μA; Fig. 3C), and 100 ms in the remainder; we found that train length had little if any effect on which cells were activated (Supp. Fig. 7).

Imaging and data collection

Imaging was performed with custom-built microscopes: Leica (Heidelberg) SP3 scan head with Mira or Chameleon laser, (Coherent Inc.), or resonant galvanometer scan head, (Electro-Optical Products Corp) with Mai Tai laser (Newport Corp.) and group delay dispersion compensator. We used a 16× 0.8NA objective (Nikon) and used excitation light of 800 or 920 nm. Frames were acquired at 2.5–31 Hz, corresponding to a time per line of 0.25–1.25 ms and a pixel dwell time of 0.4–2.5 μs. For a typical calcium decay ---exponential with time constant 2 sec (Supp. Fig. 3, Kerr et al., 2005; Greenberg et al., 2008) ---sampling at 2.5Hz will underestimate the peak response by 9% on average (e.g., from 40% peak ΔF/F, the peak is reduced to 36.8% on average).

Data analysis

Data analysis was performed with Matlab (The Mathworks). Field-of-view average images (e.g. Fig. 1B, Fig. 2A,D, etc.) were generated by averaging > 100 frames. Emitted photons

between 500–550 nm are plotted as green in these images; 550–600 nm plotted as red. Cell outlines (e.g. Fig. 6D, pink labels in Fig. 3) were identified by morphology in the averaged green image. Time courses were computed by averaging all pixels within the cell outline for each frame, and smoothed when collected at high frame rates (Fig. 2E) using a running average filter. To remove effects of bleaching or other slow variations, time courses were high-pass filtered, removing any component below about 0.02 Hz. We filtered baseline periods between each stimulus train with a kernel of 50 sec standard deviation; this moving baseline was extrapolated to the full time course and subtracted. This effected high-pass filtering and yielded what we term ΔF. Dividing by the average baseline (a scalar) gave $\Delta F/F_0$.

Image masks that shade pixels of low signal-to-noise (Fig. 4A, Fig. 6A) were computed by spatial low-pass filtering and thresholding average green images at about 10% of maximum fluorescence. Because the principal source of noise is photon shot noise, noise levels rise monotonically as pixel intensity decreases, so that masking pixels of low intensity also masks those of high noise.

We classified neurons that showed a change of >= 20% $\Delta F/F_0$ as activated by stimulation (Results; Fig 3B; Supp. Figs. 5,8). In cases when the frame time was 100–300 ms, we took the peak response to be the value from the single frame after the stimulus train, and for faster frame times of 31 ms, we computed the stimulation response from the 5 frames immediately after the stimulus train was ended (Fig. 2F). In Fig. 3C, inferred thresholds were the average of the highest current that produced zero responsive cells and the lowest current resulting in any responsive cells, except in one case where the lowest current we measured showed a response and we took that current to be the threshold.

We report $\Delta F/F_0$, even though the usual use of this measure is to quantify fluorescence changes in a focal volume in terms of the number of fluorophores in that volume (Helmchen, 1999). Quantifying this requires measurement of all background fluorescence that does not arise from the focal volume, a difficult task in bulk-loaded calcium indicator experiments (Helmchen, 1999). We use this measure because it conveniently normalizes for variation in brightness across the field of view we image. Because we do not estimate and subtract background fluorescence, we are likely underestimating $\Delta F/F_0$.

Response maps in Figs. 6A and 7C were made by computing the $\Delta F/F_0$ for each pixel; in this case the immediately preceding baseline period was subtracted from each stimulation period to give ΔF, and F_0 was the scalar average baseline. We limited the F_0 divisor to be >= 10% of the maximum fluorescence (e.g. 25ADU for an 8-bit image). This was to prevent very large values for dim, noisy pixels produced by dividing by a small baseline, while still allowing large cell responses to be seen (e.g. Fig. 6A, 10 μA panel, top right, underneath mask). The masked cell plot in Fig. 6F was made by computing the mean response of the pixels within each cell outline and then filling the entire cell outline with the color from the colormap (shown in Fig. 6A) corresponding to that mean.

Supplementary Material

Refer to Web version on PubMed Central for supplementary material.

Acknowledgments

We thank Kenichi Ohki for assistance with experiments, and Sergey Yurgenson for technical contributions. Davi Bock and Wei-Chung Lee kindly provided electron microscopic images. We also thank K.O., Marlene Cohen, John Asaad, John Maunsell, Mark Andermann, Ed Tehovnik, Lindsey Glickfeld, and Nic Price for valuable suggestions and discussion. This work was supported by NIH grants R01 EY010115, R01 EY018742, R21 NS061203, and T32 NS007484 (M.H.); and by Microsoft Research.

References

Albright TD, Desimone R, Gross CG. Columnar organization of directionally selective cells in visual area MT of the macaque. Journal of Neurophysiology 1984;51:16–31. [PubMed: 6693933]

Asanuma H, Stoney SD, Abzug C. Relationship between afferent input and motor outflow in cat motorsensory cortex. Journal of Neurophysiology 1968;31:670–681. [PubMed: 5711138]

Bak M, Girvin JP, Hambrecht FT, Kufta CV, Loeb GE, Schmidt EM. Visual sensations produced by intracortical microstimulation of the human occipital cortex. Medical & biological engineering & computing 1990;28:257–259. [PubMed: 2377008]

Berman NJ, Douglas RJ, Martin KA, Whitteridge D. Mechanisms of inhibition in cat visual cortex. J Physiol (Lond) 1991;440:697–722. [PubMed: 1804983]

Bishop PO, Burke W, Davis R. Single-unit recording from antidromically activated optic radiation neurones. J Physiol (Lond). 1962

Bizzi E. Discharge of frontal eye field neurons during eye movements in unanesthetized monkeys. Science 1967;157:1588–1590. [PubMed: 4962575]

Braitenberg V, Schüz A. Cortex: Statistics and Geometry of Neuronal Connectivity. Neuro-und Sinnesphysiologie. 2001

Bruce CJ, Goldberg ME, Bushnell MC, Stanton GB. Primate frontal eye fields. II. Physiological and anatomical correlates of electrically evoked eye movements. Journal of Neurophysiology 1985;54:714–734. [PubMed: 4045546]

Butovas S. Spatiotemporal Effects of Microstimulation in Rat Neocortex: A Parametric Study Using Multielectrode Recordings. Journal of Neurophysiology 2003;90:3024–3039. [PubMed: 12878710]

Chapin JK. Impact of neuroprosthetic applications on functional recovery. PROGRESS IN BRAIN RESEARCH 2000;128:115–120. [PubMed: 11105673]

Chung S, Ferster D. Strength and orientation tuning of the thalamic input to simple cells revealed by electrically evoked cortical suppression. Neuron 1998;20:1177–1189. [PubMed: 9655505]

Creutzfeldt OD, Watanabe S, Lux HD. Relations between EEG phenomena and potentials of single cortical cells. I. Evoked responses after thalamic and erpicortical stimulation. Electroencephalogr Clin Neurophysiol 1966;20:1–18. [PubMed: 4161317]

Deisz RA, Prince DA. Frequency-dependent depression of inhibition in guinea-pig neocortex in vitro by GABAB receptor feed-back on GABA release. J Physiol (Lond) 1989;412:513–541. [PubMed: 2557431]

Desmurget M, Reilly KT, Richard N, Szathmari A, Mottolese C, Sirigu A. Movement intention after parietal cortex stimulation in humans. Science 2009;324:811–813. [PubMed: 19423830]

Doty RW. Electrical Stimulation of the Brain in Behavioral Context. Annual Reviews in Psychology. 1969

Douglas, RJ.; Martin, KAC. Neocortex. In: Shepherd, GM., editor. The Synaptic Organization of the Brain. Oxford University Press; New York: 1998. p. 459-510.

Durand, D. The Biomedical Engineering Handbook. 2000. Electric Stimulation of Excitable Tissue.

Ekstrom LB, Roelfsema PR, Arsenault JT. Bottom-Up Dependent Gating of Frontal Signals in Early Visual Cortex. Science. 2008

Fitzsimmons NA, Drake W, Hanson TL, Lebedev MA, Nicolelis MA. Primate reaching cued by multichannel spatiotemporal cortical microstimulation. J Neurosci 2007;27:5593–5602. [PubMed: 17522304]

Fritsch G, Hitzig E. Ueber die elektrische Erregbarkeit des Grosshirns. Archiv fur Anatomie, Physiologie und wissenschaftliche Medizin 1870;37:300–339.

Galarreta M, Hestrin S. Frequency-dependent synaptic depression and the balance of excitation and inhibition in the neocortex. Nat Neurosci 1998;1:587–594. [PubMed: 10196566]

Garaschuk O, Milos RI, Grienberger C, Marandi N, Adelsberger H, Konnerth A. Optical monitoring of brain function in vivo: from neurons to networks. Pfl■gers Archiv European Journal of Physiology 2006;453:385–396.

Gilbert CD. Horizontal integration and cortical dynamics. Neuron 1992;9:1–13. [PubMed: 1632964]

Gilbert CD, Wiesel TN. Morphology and intracortical projections of functionally characterised neurones in the cat visual cortex. Nature 1979;280:120–125. [PubMed: 552600]

Gilbert CD, Wiesel TN. Columnar specificity of intrinsic horizontal and corticocortical connections in cat visual cortex. J Neurosci 1989;9:2432–2442. [PubMed: 2746337]

Glimcher PW, Sparks DL. Effects of low-frequency stimulation of the superior colliculus on spontaneous and visually guided saccades. Journal of Neurophysiology 1993;69:953–964. [PubMed: 8463820]

Göbel W, Kampa BM, Helmchen F. Imaging cellular network dynamics in three dimensions using fast 3D laser scanning. Nat Meth 2007;4:73–79.

Graziano MS, Taylor CS, Moore T. Complex movements evoked by microstimulation of precentral cortex. Neuron 2002a;34:841–851. [PubMed: 12062029]

Graziano MS, Taylor CS, Moore T, Cooke DF. The cortical control of movement revisited. Neuron 2002b; 36:349–362. [PubMed: 12408840]

Greenberg DS, Houweling AR, Kerr JN. Population imaging of ongoing neuronal activity in the visual cortex of awake rats. Nat Neurosci 2008;11:749–751. [PubMed: 18552841]

Häusser M, Major G, Stuart GJ. Differential shunting of EPSPs by action potentials. Science 2001;291:138–141. [PubMed: 11141567]

Helmchen, F. Calibration of fluorescent calcium indicators. In: Yuste, R.; Lanni, F.; Konnerth, A., editors. Imaging living cells: A laboratory manual. CSHL Press; 1999.

Helmchen F, Imoto K, Sakmann B. Ca2+ buffering and action potential-evoked Ca2+ signaling in dendrites of pyramidal neurons. Biophysical Journal 1996;70:1069–1081. [PubMed: 8789126]

Henze DA, Borhegyi Z, Csicsvari J, Mamiya A, Harris KD, Buzsáki G. Intracellular features predicted by extracellular recordings in the hippocampus in vivo. Journal of Neurophysiology 2000;84:390–400. [PubMed: 10899213]

Histed MH, Miller EK. Microstimulation of frontal cortex can reorder a remembered spatial sequence. Plos Biol 2006;4:e134. [PubMed: 16620152]

Houweling AR, Brecht M. Behavioural report of single neuron stimulation in somatosensory cortex. Nature 2008;451:65–68. [PubMed: 18094684]

Huber D, Petreanu L, Ghitani N, Ranade S, Hromádka T, Mainen Z, Svoboda K. Sparse optical microstimulation in barrel cortex drives learned behaviour in freely moving mice. Nature 2008;451:61–64. [PubMed: 18094685]

Jackson A, Mavoori J, Fetz EE. Long-term motor cortex plasticity induced by an electronic neural implant. Nature 2006;444:56–60. [PubMed: 17057705]

Johnson MD, Miocinovic S, McIntyre CC, Vitek JL. Mechanisms and targets of deep brain stimulation in movement disorders. Neurotherapeutics: the journal of the American Society for Experimental NeuroTherapeutics 2008;5:294–308. [PubMed: 18394571]

Johnston, D.; Wu, S. Foundations of Cellular Neurophysiology. MIT Press; Cambridge, MA: 1994.

Kara P, Pezaris J, Yurgenson S, Reid RC. The spatial receptive field of thalamic inputs to single cortical simple cells revealed by the interaction of visual and electrical stimulation. Proc Natl Acad Sci USA 2002;99:16261–16266. [PubMed: 12461179]

Kerr JN, Denk W. Imaging in vivo: watching the brain in action. Nat Rev Neurosci 2008;9:195–205. [PubMed: 18270513]

Kerr JN, Greenberg D, Helmchen F. Imaging input and output of neocortical networks in vivo. Proc Natl Acad Sci USA 2005;102:14063–14068. [PubMed: 16157876]

Kimmel DL, Moore T. Temporal patterning of saccadic eye movement signals. J Neurosci 2007;27:7619–7630. [PubMed: 17634356]

Lebedev MA, Nicolelis MA. Brain-machine interfaces: past, present and future. Trends in Neurosciences 2006;29:536–546. [PubMed: 16859758]

Lemon, R. Methods for Neuronal Recording in Conscious Animals. John Wiley and Sons; 1984. IBRO Handbook Series v4

Martin KA, Whitteridge D. Form, function and intracortical projections of spiny neurones in the striate visual cortex of the cat. J Physiol (Lond) 1984;353:463–504. [PubMed: 6481629]

Merrill D, Bikson M, Jefferys J. Electrical stimulation of excitable tissue: design of efficacious and safe protocols. Journal of Neuroscience Methods 2005;141:171–198. [PubMed: 15661300]

Moeller S, Freiwald WA, Tsao DY. Patches with links: a unified system for processing faces in the macaque temporal lobe. Science 2008;320:1355–1359. [PubMed: 18535247]

Moore T, Fallah M. Control of eye movements and spatial attention. Proc Natl Acad Sci USA 2001;98:1273–1276. [PubMed: 11158629]

Moore T, Fallah M. Microstimulation of the frontal eye field and its effects on covert spatial attention. Journal of Neurophysiology 2004;91:152–162. [PubMed: 13679398]

Movshon JA, Newsome WT. Visual response properties of striate cortical neurons projecting to area MT in macaque monkeys. J Neurosci 1996;16:7733–7741. [PubMed: 8922429]

Mrsic-Flögel TD, Hofer SB, Ohki K, Reid RC, Bonhoeffer T, Hübener M. Homeostatic regulation of eye-specific responses in visual cortex during ocular dominance plasticity. Neuron 2007;54:961–972. [PubMed: 17582335]

Murasugi CM, Salzman CD, Newsome WT. Microstimulation in visual area MT: effects of varying pulse amplitude and frequency. J Neurosci 1993;13:1719–1729. [PubMed: 8463847]

Murphey DK, Maunsell JH. Behavioral detection of electrical microstimulation in different cortical visual areas. Curr Biol 2007;17:862–867. [PubMed: 17462895]

Murphey DK, Maunsell JH. Electrical microstimulation thresholds for behavioral detection and saccades in monkey frontal eye fields. Proc Natl Acad Sci USA 2008;105:7315–7320. [PubMed: 18477698]

Nimmerjahn A, Kirchhoff F, Kerr JN, Helmchen F. Sulforhodamine 101 as a specific marker of astroglia in the neocortex in vivo. Nat Meth 2004;1:31–37.

Nowak LG, Bullier J. Axons, but not cell bodies, are activated by electrical stimulation in cortical gray matter. I. Evidence from chronaxie measurements. Experimental brain research Experimentelle Hirnforschung Expérimentation cérébrale 1998a;118:477–488.

Nowak LG, Bullier J. Axons, but not cell bodies, are activated by electrical stimulation in cortical gray matter. II. Evidence from selective inactivation of cell bodies and axon initial segments. Experimental brain research Experimentelle Hirnforschung Expérimentation cérébrale 1998b;118:489–500.

Ohki K, Chung S, Ch'ng YH, Kara P, Reid RC. Functional imaging with cellular resolution reveals precise micro-architecture in visual cortex. Nature 2005;433:597–603. [PubMed: 15660108]

Penfield W. Ferrier Lecture: Some Observations on the Cerebral Cortex of Man. Proceedings of the Royal Society of London Series BBiological Sciences 1947:329–347.

Pezaris J, Reid RC. Demonstration of artificial visual percepts generated through thalamic microstimulation. Proc Natl Acad Sci USA 2007;104:7670–7675. [PubMed: 17452646]

Ranck JB. Which elements are excited in electrical stimulation of mammalian central nervous system: a review. Brain Res. 1975

Rathelot JA, Strick PL. Muscle representation in the macaque motor cortex: an anatomical perspective. Proc Natl Acad Sci USA 2006;103:8257–8262. [PubMed: 16702556]

Rattay F. The basic mechanism for the electrical stimulation of the nervous system. Neuroscience 1999;89:335–346. [PubMed: 10077317]

Robinson DA, Fuchs AF. Eye movements evoked by stimulation of frontal eye fields. Journal of Neurophysiology 1969;32:637–648. [PubMed: 4980022]

Rockland KS, Lund JS. Widespread periodic intrinsic connections in the tree shrew visual cortex. Science 1982;215:1532–1534. [PubMed: 7063863]

Romo R, Hernández A, Zainos A, Salinas E. Somatosensory discrimination based on cortical microstimulation. Nature 1998;392:387–390. [PubMed: 9537321]

Salzman CD, Britten KH, Newsome WT. Cortical microstimulation influences perceptual judgements of motion direction. Nature 1990;346:174–177. [PubMed: 2366872]

Salzman CD, Murasugi CM, Britten KH, Newsome WT. Microstimulation in visual area MT: effects on direction discrimination performance. J Neurosci 1992;12:2331–2355. [PubMed: 1607944]

Sato TR, Gray NW, Mainen ZF, Svoboda K. The Functional Microarchitecture of the Mouse Barrel Cortex. Plos Biol 2007;5:e189. [PubMed: 17622195]

Schiller PH, Tehovnik EJ. Visual prosthesis. Perception 2008;37 advance online publication; Oct 10 2008.

Schlag JD, Schlag-Rey M. Evidence for a supplementary eye field. Journal of Neurophysiology 1987;57:179–200. [PubMed: 3559671]

Schmidt EM, Bak MJ, Hambrecht FT, Kufta CV, O'Rourke DK, Vallabhanath P. Feasibility of a visual prosthesis for the blind based on intracortical microstimulation of the visual cortex. Brain 1996;119 (Pt 2):507–522. [PubMed: 8800945]

Schummers J, Yu H, Sur M. Tuned responses of astrocytes and their influence on hemodynamic signals in the visual cortex. Science 2008;320:1638–1643. [PubMed: 18566287]

Silver RA, Lubke J, Sakmann B, Feldmeyer D. High-probability uniquantal transmission at excitatory synapses in barrel cortex. Science 2003;302:1981–1984. [PubMed: 14671309]

Smetters D, Majewska A, Yuste R. Detecting action potentials in neuronal populations with calcium imaging. Methods 1999;18:215–221. [PubMed: 10356353]

Sohya K, Kameyama K, Yanagawa Y, Obata K, Tsumoto T. GABAergic Neurons Are Less Selective to Stimulus Orientation than Excitatory Neurons in Layer II/III of Visual Cortex, as Revealed by In Vivo Functional Ca2+ Imaging in Transgenic Mice. Journal of Neuroscience 2007;27:2145–2149. [PubMed: 17314309]

Sommer MA, Wurtz RH. A pathway in primate brain for internal monitoring of movements. Science 2002;296:1480–1482. [PubMed: 12029137]

Stanford TR, Freedman EG, Sparks DL. Site and parameters of microstimulation: evidence for independent effects on the properties of saccades evoked from the primate superior colliculus. Journal of Neurophysiology 1996;76:3360–3381. [PubMed: 8930279]

Stoney SD, Thompson WD, Asanuma H. Excitation of pyramidal tract cells by intracortical microstimulation: effective extent of stimulating current. Journal of Neurophysiology 1968;31:659–669. [PubMed: 5711137]

Stosiek C, Garaschuk O, Holthoff K, Konnerth A. In vivo two-photon calcium imaging of neuronal networks. Proc Natl Acad Sci USA 2003;100:7319–7324. [PubMed: 12777621]

Stratford KJ, Tarczy-Hornoch K, Martin KA, Bannister NJ, Jack JJ. Excitatory synaptic inputs to spiny stellate cells in cat visual cortex. Nature 1996;382:258–261. [PubMed: 8717041]

Strick PL. Stimulating research on motor cortex. Nat Neurosci 2002;5:714–715. [PubMed: 12149622]

Stuart, G.; Spruston, N.; Häusser, M. Dendrites. Oxford University Press; New York: 2000.

Stuart G, Spruston N, Sakmann B, Häusser M. Action potential initiation and backpropagation in neurons of the mammalian CNS. Trends in Neurosciences 1997;20:125–131. [PubMed: 9061867]

Taylor CS, Gross CG. Twitches versus movements: a story of motor cortex. The Neuroscientist: a review journal bringing neurobiology, neurology and psychiatry 2003;9:332–342.

Tehovnik EJ. Electrical stimulation of neural tissue to evoke behavioral responses. Journal of Neuroscience Methods 1996;65:1–17. [PubMed: 8815302]

Tehovnik EJ, Slocum WM. Phosphene induction by microstimulation of macaque V1. Brain research reviews 2007;53:337–343. [PubMed: 17173976]

Tehovnik EJ, Tolias AS, Sultan F, Slocum WM, Logothetis NK. Direct and indirect activation of cortical neurons by electrical microstimulation. Journal of Neurophysiology 2006;96:512–521. [PubMed: 16835359]

Thomson AM, Deuchars J. Temporal and spatial properties of local circuits in neocortex. Trends in Neurosciences 1994;17:119–126. [PubMed: 7515528]

Tolias A, Sultan F, Augath M, Oeltermann A, Tehovnik EJ, Schiller P, Logothetis N. Mapping Cortical Activity Elicited with Electrical Microstimulation Using fMRI in the Macaque. Neuron 2005;48:901–911. [PubMed: 16364895]

Ts'o DY, Gilbert CD, Wiesel TN. Relationships between horizontal interactions and functional architecture in cat striate cortex as revealed by cross-correlation analysis. J Neurosci 1986;6:1160–1170. [PubMed: 3701413]

Varela JA, Sen K, Gibson J, Fost J, Abbott LF, Nelson SB. A quantitative description of short-term plasticity at excitatory synapses in layer 2/3 of rat primary visual cortex. J Neurosci 1997;17:7926–7940. [PubMed: 9315911]

Vitek JL. Mechanisms of deep brain stimulation: excitation or inhibition. Mov Disord 2002;17(Suppl 3):S69–72. [PubMed: 11948757]

Williams ZM, Eskandar EN. Selective enhancement of associative learning by microstimulation of the anterior caudate. Nat Neurosci 2006;9:562–568. [PubMed: 16501567]

Yaksi E, Friedrich RW. Reconstruction of firing rate changes across neuronal populations by temporally deconvolved Ca2+ imaging. Nat Meth 2006;3:377–383.

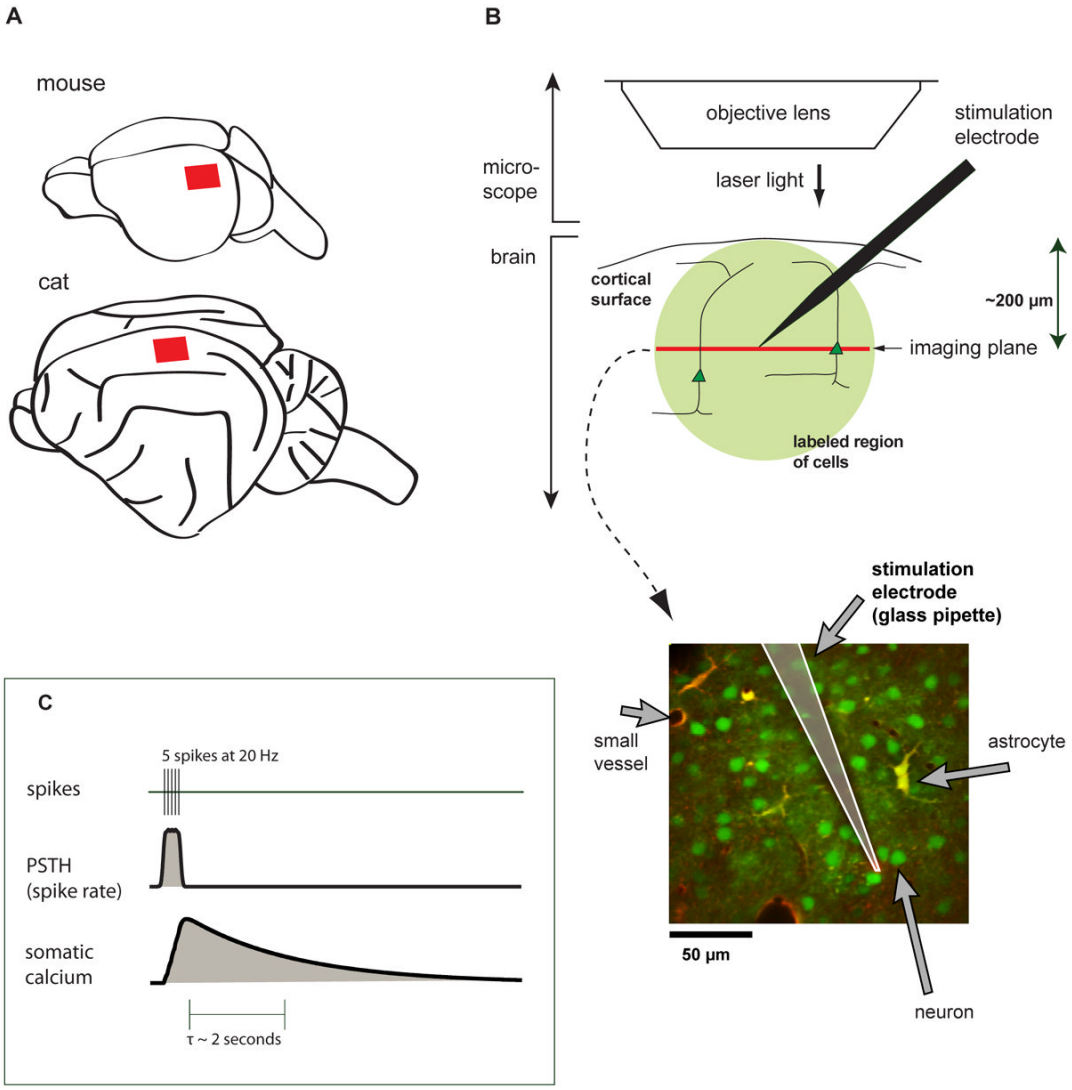

Figure 1. Using two-photon imaging to measure the effects of cortical microstimulation

(A) Schematic location of imaging sites in cortex, primary visual cortex of mouse, rat (not shown), and cat (area 18).

(B) Two-photon bulk-loaded calcium imaging *in vivo*. Femtosecond-pulsed laser light is used to measure calcium-induced fluorescence changes in neurons. A single plane is imaged at one time. Lower panel: example image. All cells are loaded with OGB-1 AM (green), and astrocytes are labeled with SR101 (red/yellow).

(C) Relationship between calcium concentration and spiking activity. Top: a simulated train of 5 spikes. Middle: spike rate, computed by smoothing the spike train with a Gaussian kernel. Bottom: expected somatic calcium concentration, computed by convolving an exponential describing calcium influx with the spike train.

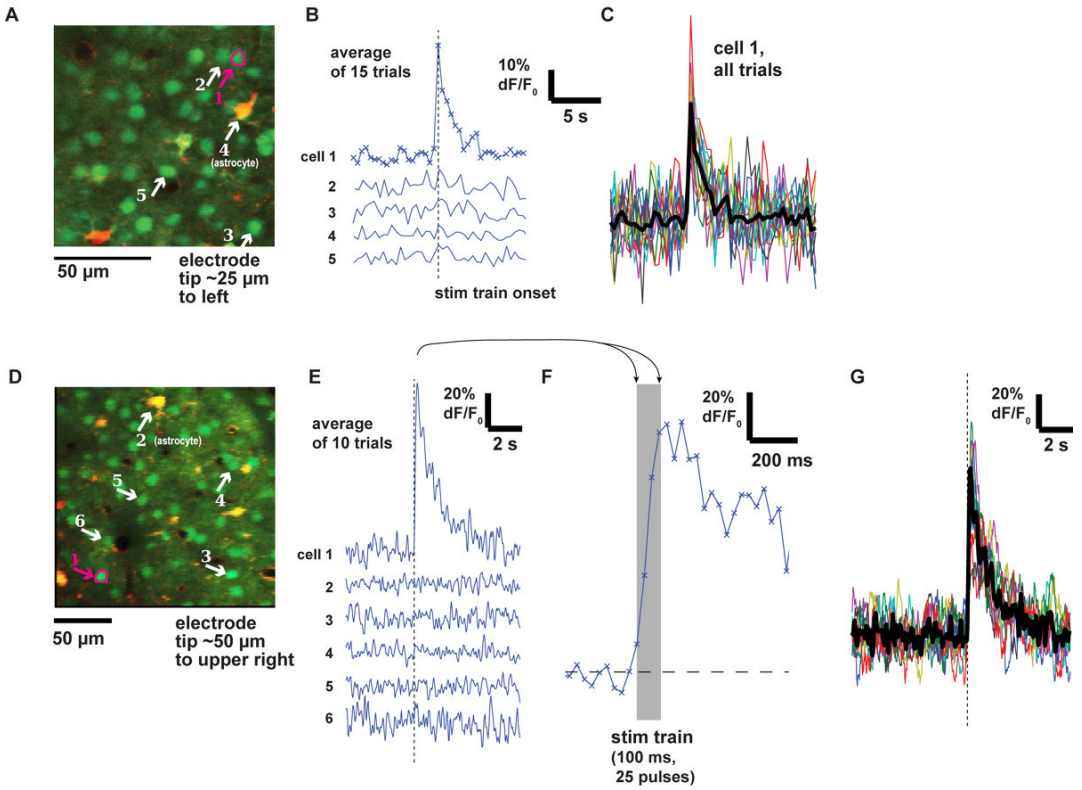

Figure 2. Measured time courses in neurons in response to microstimulation

(A) Anatomical view of neurons and astrocytes in mouse visual cortex. Electrode is positioned 25 µm to right of image. Arrows point to somas of 5 cells: four neurons (1,2,3,5) and one astrocyte (4). Image frames were collected at 2.5 Hz.

(B) Time courses (average of 15 repetitions) of the differential fluorescence signal ($\Delta F/F_0$) from the 5 cells labeled in (A). Only cell 1 responded. Stimulation with glass pipette: 100 ms train, 16 µA.

(C) Time courses of single trial responses from cell 1 in (A). Each of 15 repetitions is plotted in a single color and the mean is plotted in black.

(D–E) As in (A–B), for a second experiment in mouse visual cortex. Here image frames were collected at 31 Hz. Stimulation with glass pipette: 100 ms train at 10 µA.

(F) Expanded view of cell 1's average trace in (E).

(G) Time courses of individual trials from cell 1 in (E,F). Conventions as in (C).

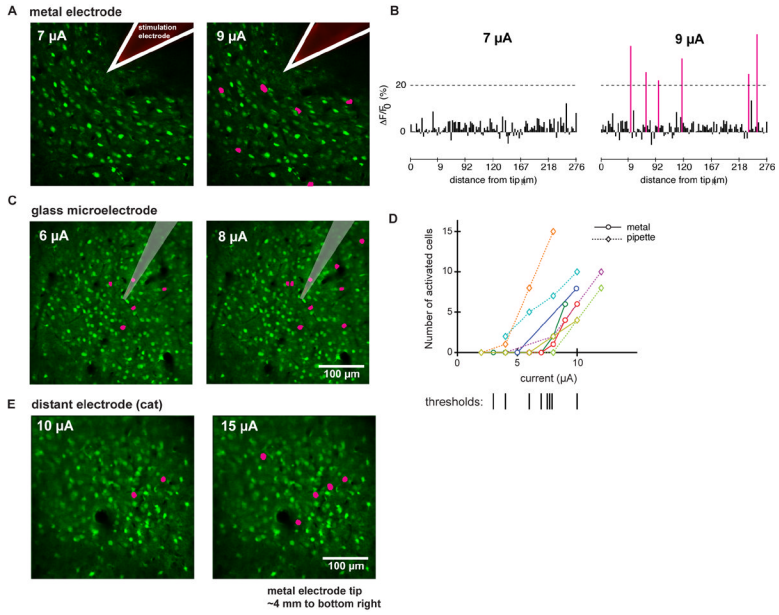

Figure 3. The pattern of activated cells is sparse

(A) Anatomical images with overlay showing activated neurons for two currents; metal electrode, cat area 18. Pink indicates cells with greater than 20% $\Delta F/F_0$ average response. While no cells are activated at 7 μA, several are activated at 9 μA.

(B) Average $\Delta F/F_0$ responses of all cells for experiment in (A). Pink bars are cells that showed greater than 20% $\Delta F/F_0$ average responses.

(C) As in (A); glass pipette, mouse visual cortex. Number of activated cells increases with current.

(D) Summary of 8 experiments in which current was systematically changed. X-axis, current. Y-axis, number of cells activated in imaging plane. Dotted lines: stimulation applied with pipette; solid lines, metal electrode. Bottom: vertical lines show inferred threshold for each experiment.

(E) As in (A, C); metal electrode, cat area 18. Electrode was positioned 4 mm away, to bottom right of image.

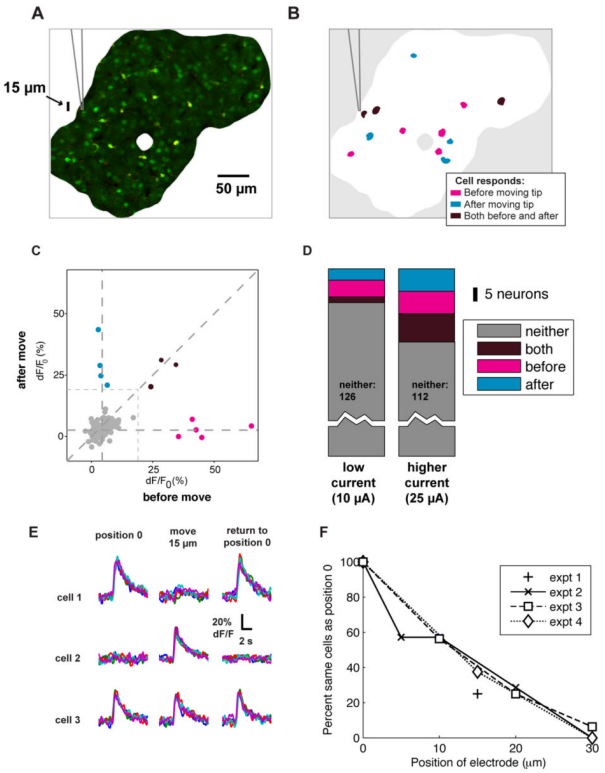

Figure 4. Moving the tip slightly yields a different set of activated cells

(A) Image showing the position of cells relative to the electrode. Only the region well-loaded by the calcium indicator is shown. Glass pipette, mouse visual cortex.

(B) Schematic diagram indicating which cells were activated by stimulation before and after withdrawing the electrode by 15 µm. While some cells respond both before and after moving the tip (purple), many respond exclusively before (magenta) or after (cyan). Note: cell outlines enlarged for clarity. Stimulation: 100 ms train at 10 µA (interleaved with 25 µA trains, results shown in D).

(C) Responses of all cells, before and after moving the tip. X-axis: average $\Delta F/F_0$ response before moving the electrode. Y-axis: response to stimulation after the tip was moved. Gray data points did not reach activation threshold. Others colored as in (B).

(D) Distribution of responses for low current (A–C) and high current (25 µA) conditions. Higher currents activate more cells, with more overlap between *before* and *after* populations.

(E) Time courses of responses for another experiment in which electrode was moved 15 µm away and then repositioned to its original location. Individual trials shown as different colors. Glass pipette, mouse visual cortex. Stimulation: 100 ms train at 12 µA. Three example cells are shown here, out of 136 imaged cells. A total of 7 cells were activated at position 0 (*left)*, 14 at the deeper position (*middle)* and 8 when tip was returned to position 0 *(right)*. Of these, 1 cell active at position 0 was no longer activated on return to position 0, and two additional cells were activated, presumably because the electrode was not restored to the exact same (micron-level precision) position in the tissue.

(F) Fraction of cells activated at both electrode positions as a function of displacement, for four experiments (expt. 1 – 4). Expt.. 1 is data in (B–C). Expts. 2 – 4 are control experiments in which displacement was increased from 5 to 30 µm. All experiments were done at near-threshold currents (10, 12 and 10 µA). Fraction at position 0 is defined at 100%.

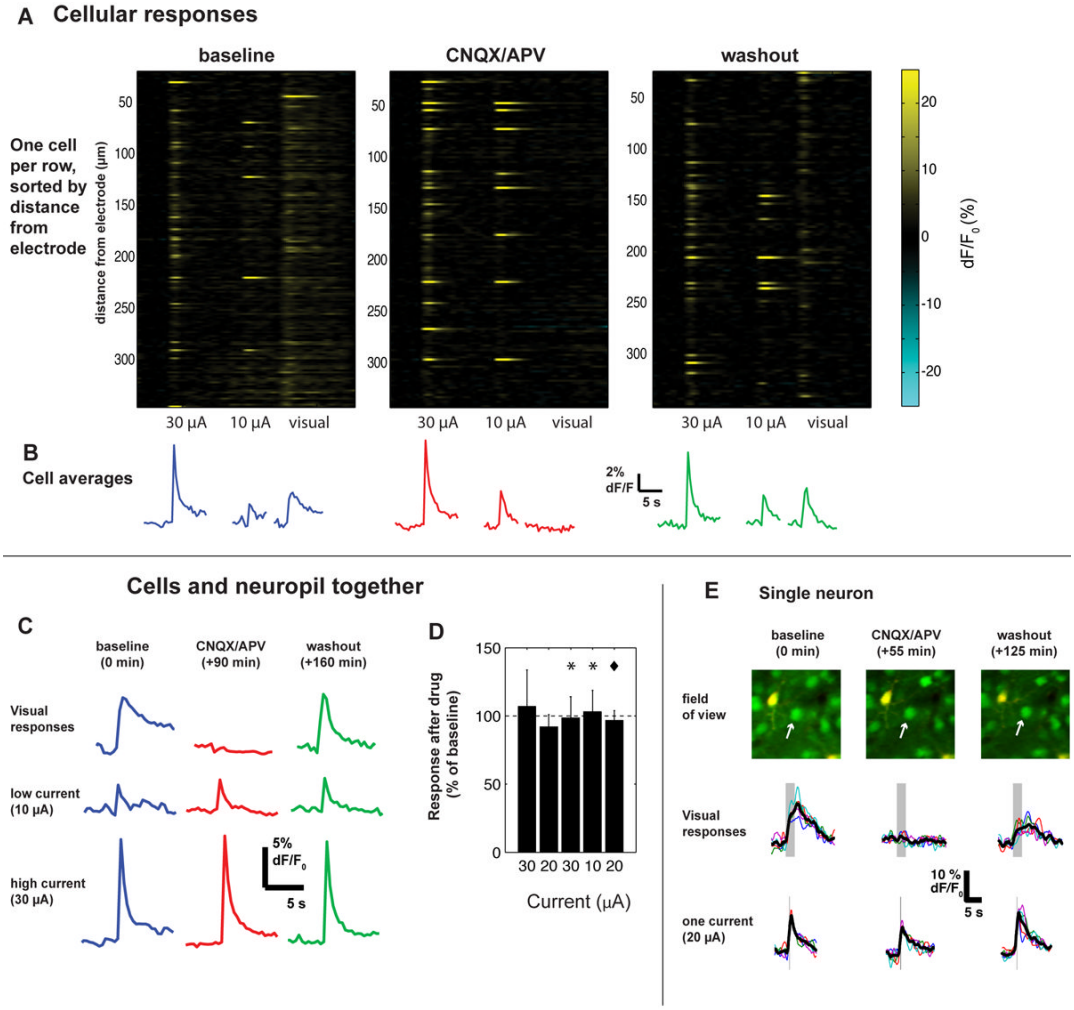

Figure 5. Activation is similar after blocking excitatory transmission

(A) Cellular responses before (left), during (center), and after (right) blockade of excitatory glutamatergic synapses with CNQX and APV. Each row shows the responses of a single cell. Visual stimulus was a drifting square-wave grating in a direction (0 deg) chosen to most strongly excite this region. Electrical stimulus was a 100 ms train at 250 Hz.

(B) Average time courses of all cells shown in B. Responses to visual stimuli were abolished by drug application but responses to electrical stimulation were left intact. Note that electrical responses are larger than visual responses; the amplitude of the visual response is consistent with earlier work (Ohki et al., 2005; Sohya et al., 2007).

(C) Time course of responses during drug application. Here we averaged $\Delta F/F_0$ responses over neuropil and all cells in the imaged region to be resistant to small pipette movements.

(D) Results from 3 experiments (visual cortex; 1 mouse, 2 cats). Y-axis: percent change between pre-drug baseline and drug application of $\Delta F/F_0$ responses to microstimulation, averaged over entire imaged region. Error bars: 3 standard deviations. Dashed line indicates no change. Stars (*) indicate results from experiment in (A–C); diamond, results from experiment in (E).

(E) Control experiment in which the same cells were imaged throughout the experiment. Stimulation: 100 ms trains at 25 μA.

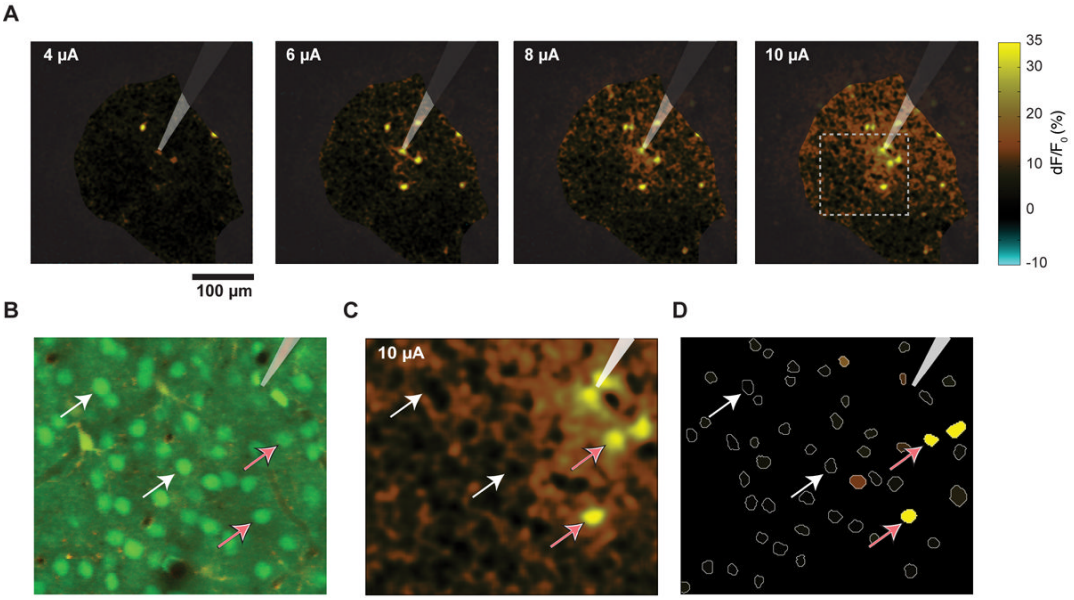

Figure 6. Many cells show large responses or no response, while neuropil activation is homogeneous

(A) Maps of activation as current is increased; $\Delta F/F_0$ was calculated on a per-pixel basis and shown for all pixels (color scale shown at right). Same experiment as shown in Figs 3B and 5. Stimulation train: 100 ms.

(B) Enlarged view of area indicated with dotted line in A, 10 μA (rightmost panel of A). Shown here is the average anatomy image, with neurons green and astrocytes red/yellow. Electrode tip is visible at top right.

(C) $\Delta F/F_0$ map, same region shown in B and indicated with dotted line in A. White arrows: non-activated cells; pink arrows: cells that respond strongly to stimulation. Color scale as in A. Note the activated neuropil region immediately around the tip, which is masked by two less-active cells, one on each side.

(D) Panel showing our method for computing cell responses: cells (white lines) were identified from anatomy image. Average $\Delta F/F_0$ value was computed within each white region and plotted here in color. Electrode tip position and pink and white arrows, same conventions as B, C. Same color scale as A and C.

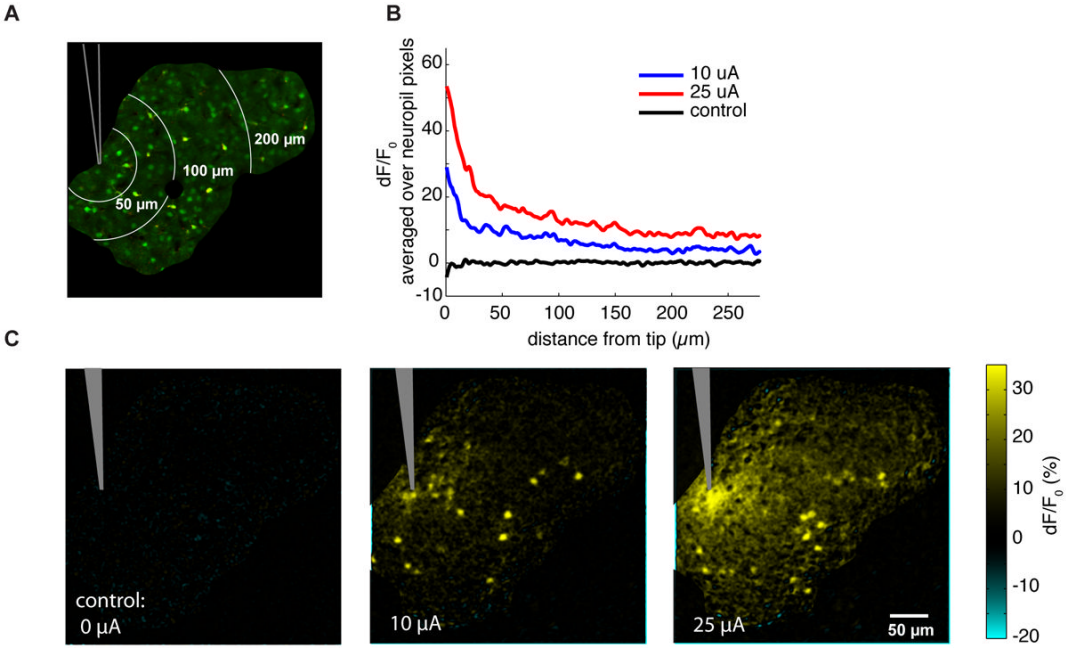

Figure 7. Neuropil activation shows a slow spatial falloff

(A) Anatomical image, with high signal-to-noise area indicated by black outline. Mouse visual cortex, glass pipette, same experiment as in Fig. 4. White lines indicate contours of constant distance from the tip.

(B) Neuropil response, plotted as a function of distance from the tip. X-axis, distance from tip; Y-axis, $\Delta F/F_0$, averaged over all pixels in the neuropil at that distance; cell regions are masked out. Note the large neuropil peak near the tip, and the slow falloff at larger distances.

(C) Response as current is increased. Color scale: average $\Delta F/F_0$ response to 30 repetitions of stimulation.

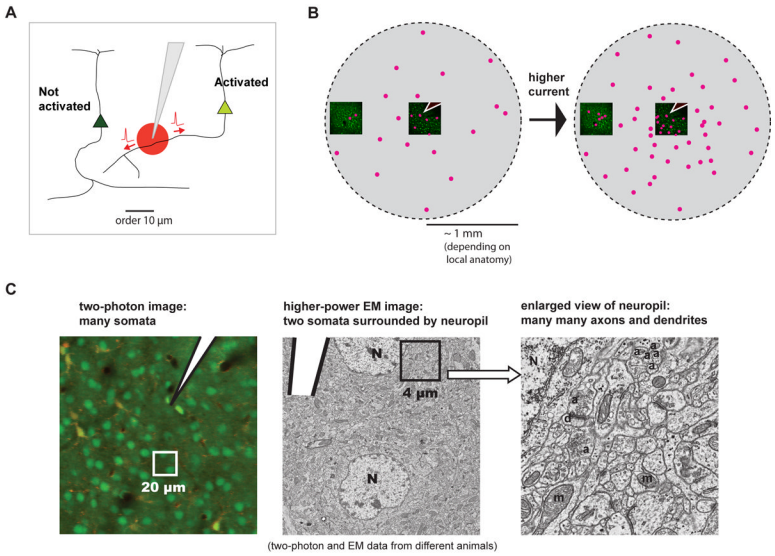

Figure 8. Model of cell recruitment by local axonal activation

(A) Model of effects at small scales. A small region of directly-activated neural processes near the tip yields sparse activated cell bodies at a distance.

(B) Model of effects at large scales. Activating processes near the tip gives a ball of activated cells, but even near threshold this ball is sparse. Increasing current causes the ball to fill in as more cells are activated throughout.

(C) Schematic showing the large number of potential axons near the electrode tip. Left, two-photon anatomy image showing neural cell bodies, electrode (white) and neuropil regions between cell somata. Middle: electron micrograph of a 20 µm square region of mouse cortex, *from a different animal.* Pipette tip is shown schematically and drawn to approximate scale; two cell bodies are labeled. Right: an enlarged view of a 4 micron square region. N, nuclei; d, dendrites; a, probable axons; m, mitochondria.